Microwave Imaging of Non-Weak Targets via Compressive Sensing and Virtual Experiments

M. T. Bevacqua, L. Crocco, *Senior Member, IEEE*, L. Di Donato and T. Isernia, *Member IEEE*

***Abstract* — Compressive Sensing based techniques can represent a very attractive approach to inverse scattering problems. In fact, if the unknown has a sparse representation and the measurements are properly organized, CS allows to considerably reduce the number of measurements and offers the possibility to achieve optimal (or nearly optimal) reconstruction performance. Unfortunately, the inverse scattering problem is non linear, while CS theory is well established only for linear recovery problems. As a contribution to overcome this issue, in this letter, we introduce two different CS inspired approaches that exploit the "virtual experiments" framework in order to formulate the inverse scattering problems within a linear framework even in the case of non-weak targets.**

***Index Terms*—Compressive Sensing, Inverse Scattering Problem, L_1 - norm minimization, Virtual Experiments, Total Variation.**

I. Introduction and Motivations

Compressive sensing (CS) [1,2] is an emerging framework for data acquisition and signal recovery based on the concept of *sparsity*, where a signal is said to be sparse in a given basis, if it can be exactly represented by means of a few non-zero elements. A related concept is *compressibility*. Roughly speaking, a signal is said to be compressible in a given basis if it can be represented, without any significant information loss, by a few non-zero elements. Notably, in both cases one does not know a priori which elements of the representation are different from zero.

Microwave imaging could in principle take significant profit from CS techniques, since in a wide range of applications, ranging from subsurface imaging to non-destructive testing and biomedical imaging, the sought unknown can be assumed to be sparse (or compressible) in a suitable basis.

On the other hand, two relevant issues must be faced for the application of CS theories and procedures: the choice of a convenient representation basis for the specific problem at hand, and the intrinsic non-linear nature of the electromagnetic inverse scattering problem. As a consequence, the exploitation of CS in inverse scattering has been generally restricted to cases where the scatterers are both sparse in space (point-like) and "weak", so that the Born approximation (BA) can be safely used [3]. More recent contributions have also investigated the possibility to take advantage from CS under the Rytov approximation [4] or the Distorted Born Iterative scheme [5], but their validity remains still limited. More recently [6] the joint exploitation of CS, BA and total variation (TV) has been proposed to image extended targets, but very low contrast profile are still in order.

In this letter, we show that it is possible to significantly enlarge the range of applicability of CS to inverse scattering problems, by relying on our recently introduced "virtual experiments" framework [7]. In fact, by means of a proper pre-processing and re-arranging of the scattering experiments, the virtual experiments framework allows to introduce a new effective field approximation. This latter allows to tackle the inverse scattering problem within a linear framework, which goes well beyond the range of validity of the weak scattering approximations, as it is implicitly ruled by the target at hand.

The paper is organized as follows. In Section II the scattering approximation used to linearize the inverse problem is introduced. In Section III, two different CS based approaches are presented. Finally, in Section IV numerical analysis with simulated data is reported in order to assess performances of the proposed inversion strategies. Conclusions follow. Throughout the paper, the canonical 2D scalar problem is considered and a $exp(j\omega t)$ time harmonic factor assumed and dropped.

II. Linear Approximation of The Inverse Scattering Problem via Virtual Scattering Experiments

Let us consider an unknown nonmagnetic object embedded in a homogeneous medium of known electromagnetic features and whose cross section (with compact support) Σ is hosted in the imaging domain Ω. The scatterer is probed by means of a set of incident fields transmitted by some antennas located in the far-field of Ω on a closed curve Γ. The resulting scattered

This is the post-print version of the following article: Bevacqua, M.; Crocco, L.; Di Donato, L.; Isernia, T., "Microwave Imaging of Non-Weak Targets via Compressive Sensing and Virtual Experiments," IEEE Antennas and Wireless Propagation Letters, pp.1035-1038, 2015. Article has been published in final form at: http://ieeexplore.ieee.org/document/6971164.

1536-1225 © 2015 IEEE. Personal use of this material is permitted. Permission from IEEE must be obtained for all other uses, in any current or future media, including reprinting/republishing this material for advertising or promotional purposes, creating new collective works, for resale or redistribution to servers or lists, or reuse of any copyrighted component of this work in other works.

fields are measured by receiver antennas also located on Γ. For the 2D scalar case at hand, the equations describing the scattering phenomenon for the generic v-th incident field are:

$$E_{scat}{}^{(v)}(\boldsymbol{r}) = \mathcal{A}_e\left[\chi(\boldsymbol{r}')E^{(v)}(\boldsymbol{r}')\right],\ \boldsymbol{r} \in \Gamma \qquad (1)$$

$$E^{(v)}(\boldsymbol{r}) = E_{inc}{}^{(v)}(\boldsymbol{r}) + \mathcal{A}_i\left[\chi(\boldsymbol{r}')E^{(v)}(\boldsymbol{r}')\right], \boldsymbol{r} \in \Omega \quad (2)$$

where $\boldsymbol{r} = (\boldsymbol{x}, \boldsymbol{y})$, $\boldsymbol{r}' = (\boldsymbol{x}', \boldsymbol{y}')$, $E_{inc}{}^{(v)}(\cdot)$, $E^{(v)}(\cdot)$ and $E_{scat}{}^{(v)}(\cdot)$ are the incident field, the total field in Ω, and the scattered field in Γ, respectively, $\mathcal{A}_e$ and $\mathcal{A}_i$ are a short notation for the integral radiation operators.

Eqs. (1)-(2) have then to be solved in the inverse problem in order to estimate the contrast function χ from the measured scattered fields. This problem is non linear, as the total field also depends on the unknown contrast. Moreover, whatever the measurement set-up, only a bounded amount of non-redundant information is available [8,9], so that only a finite number of independent probing fields (and measurements) will be actually exploited in the inversion [8, 9].

In order to cope with a convenient linearized model outperforming the weak scattering approximation, so that performances of CS recovery procedures are hopefully boosted, we adopt a new scattering approximation which holds true in properly designed virtual scattering experiments [7].

These latter take advantage from the linearity of the scattering phenomena (and Maxwell equations) with respect to the primary sources, and they can be easily built as follows. First, rearrange with known coefficients, say α_v, the set of the incident fields used in the different scattering experiments (see eq. 1), and sum the different fields. By so doing, a virtual incident field is designed, whose corresponding scattered field is just the superposition (with the same coefficients α_v) of the original scattered fields. By repeating such a procedure one is able to build new experiments without additional physical measurements. Obviously, the new experiments cannot contain more information than the original ones.

Then, the problem arises of how to build the virtual experiments in some convenient fashion. The basic idea is to design the scattering experiments in such a way to enforce some given behavior for the total internal field.

In [7], the basic equation of the popular algorithm of the Linear Sampling Method [10], the so-called far field equation, is exploited to build a set of virtual incident fields. The far field equation reads as:

$$\sum_{v=1}^{N} \alpha_v\, E_{scat}{}^{(v)}(\underline{R}) = H_0^{(2)}(k_b|\underline{R} - \underline{r}_s|) \qquad (3)$$

wherein $\underline{R} = (R, \varphi)$ denotes the point on Γ where receivers are placed and the right hand term is the field radiated by an elementary source placed in the generic *sampling* point $\underline{r}_s \in \Omega$. After solving eq. (3) in the whole imaging domain Ω, one selects a subset of sampling points for which a regularized solution can be actually pursued (and which according to LSM theory are expected to belong to the scatterer support [7,10-11]). By referring to these latter as the "pivot" points $\underline{r}_p$, one can then introduce a new approximation for the total field, which is given by:

$$\tilde{E}_{tot,s}(r, r_p) = \sum_{v=1}^{N} \alpha_v\, E_{inc}(r, \vartheta_v) + LP\{H_0^{(2)}(k_b|r - r_p|)\} \qquad (4)$$

wherein the second addendum is a low pass filtered version of the elementary field having singularity in the origin of the pivot point. Expression (4) asserts that the total field can be approximated as the contribution of the original incident fields as ruled by the coefficients α_v (estimated via LSM, and so "target dependent") plus the elementary field pattern originating at the pivot point, which accounts for the fact that the LSM enforces the probed targets to behave as point-like scatterers [11]. Note the singularity in each $\underline{r}_p$ is taken into account via the low pass filtering of the Green's function.

Through approximation (4) we are able to reduce the original problem (1,2) to a linear one, which allows to take advantage from CS theoretical results and procedures.

III. Solution Approaches Exploiting the Concept of "Sparsity"

The approximation (4) allows to rearrange the different data equations (1) corresponding to the different pivot points in a system of linear equations that can be formally expressed as:

$$\boldsymbol{y} = \boldsymbol{A}\,\boldsymbol{\chi} \qquad (5)$$

where $\boldsymbol{y}$ is the $M \times 1$ data vector, which contains the measured scattered fields arising in the virtual scattering experiments, $\boldsymbol{\chi}$ is the vector unknown function of the problem, i.e., the contrast function, organized into an $N \times 1$ dimensional vector, and, finally, $\boldsymbol{A}$ is the $M \times N$ matrix which relates the unknown vector to the data vector and, assuming the usual CS terminology, it represents the sensing matrix.

According to CS theory, provided the unknown is sparse in a given basis, and the matrix $\boldsymbol{A}$ fulfills given properties, it is possible to exactly solve the inverse problem even if the number of independent equations M' (note $M' \leq M$) is (much) less than N but it is sufficiently larger than S, where S is the number of coefficients of the representation different from zero. By leaving aside the discussion of which properties should be satisfied by the matrix $\boldsymbol{A}$, which is outside of the scope of this letter, we note that numerical experiments in canonical cases suggest that a successful reconstruction is achieved in more than 50% of the cases when $M' \geq 4S$, and in more than 90% of the cases when $M' \geq 8\,S$ [1,2].

A. CS approach for point-like scatterers

In a number of applications (including for example contrast agent aided breast cancer imaging [12,13], intra-wall imaging of large areas [14], differential imaging [15]) one can assume that the unknown targets are small and localized. In these cases, the unknown of the problem can be assumed to be sparse in the usual pixel based representation. In these cases, following [1,2], problem (5) can be formulated as:

$$\min_{\boldsymbol{\chi}}\{\|\boldsymbol{\chi}\|_{\ell_1}\}$$
$$subject\ to \quad \|\mathbf{A}\boldsymbol{\chi}-\mathbf{y}\|_{\ell_2} \le \delta \qquad (6)$$

where $\boldsymbol{\chi}$ is the contrast function represented in pixel basis and $\|\cdot\|_{\ell_1}$ is the $\boldsymbol{\ell_1}$ norm [1,2]. This problem is known as Basis Pursuit denoising (BPDN) or LASSO problem [16]. Note the parameter δ depends on the level of required accuracy, on the level of noise on the data and on the model error introduced by the field approximation through eq. (4).

B. CS and Total Variation for extended high-contrast scatterers

When the targets cannot be assumed to be small with respect to the probing wavelength, one may have the a priori information that the contrast profile is piecewise constant. This happens indeed in a number of cases including NDT evaluation, sub-surface sensing, geophysical probing, as well as a number of biomedical scenarios. In these cases, one can conveniently assume that the gradient of the contrast is sparse [17]. Accordingly, problem (6) can be cast as:

$$\min_{\boldsymbol{\chi}}\left\{\|\nabla_x\boldsymbol{\chi}\|_{\ell_1}+\left\|\nabla_y\boldsymbol{\chi}\right\|_{\ell_1}\right\}$$
$$subject\ to \quad \|\mathbf{A}\boldsymbol{\chi}-\mathbf{y}\|_{\ell_2} \le \delta \qquad (7)$$

Roughly speaking, the optimization problem now amounts to look for a solution whose gradient has the minimum $\boldsymbol{\ell_1}$ norm among all the contrast functions fulfilling (within a given error) the data equation (5). The similar basic idea of exploiting the sparsity of the gradient in microwave imaging has been recently used in [6], wherein, however, the range of applicability is limited to weak scatterers.

IV. Implementation and Numerical Analysis

The proposed inversion procedure is made of two steps.

The first step entails the linearization of eq. (1). In this step, by means of the LSM equation's solution and exploiting the estimated support, a set of virtual experiments are built by considering a subset of pivot points evenly spaced within the estimated scatterer's support. Then, for each of these virtual experiments, the data equation is recast (and hence linearized) through the approximation (4). It is worth to note that the support estimation of the unknown target is also exploited to a priori choose the best approach between the two above introduced. As a matter of fact, the support estimate allows to recognize if the scatterers are point-like or not, and hence to choose the most suitable approach.

In the second step, once the problem is recast as a linear one, we solve the optimization task via approaches described in eqs. (6) or (7). It is worth noting that a non-trivial issue is the choice of the tolerance parameter δ. In this respect, as one is looking for a solution different from the null vector, a possible way to address the problem is to set the parameter δ in such a way to fulfill a lower bound $\delta < \|\boldsymbol{y}\|_{\ell_2}$. Accordingly, in performing the numerical analysis, we experienced the opportunity to set δ such that $\frac{1}{10}\|\boldsymbol{y}\|_{\ell_2} \le \delta < \|\boldsymbol{y}\|_{\ell_2}$, as trade-off between the reconstruction accuracy and the feasibility of the optimization task.

In order to show the performance achievable with the proposed approaches, we report some numerical examples, dealing with simulated data. One or more unknown objects are embedded into a square imaging domain Ω of side L, and, following [8], a number of receivers M equal to the transmitters N are considered. Both transmitters and receivers are located on a circumference Γ of radius $R = 4\lambda$, and the number of cells N_c of the discretized domain is chosen according to the Richmond's rule [18]. Furthermore, the scattered field data, simulated by means of a full wave forward solver based on the method of moments, are corrupted with a random Gaussian noise with different SNR levels. To evaluate the accuracy of the retrieved contrast function, we use the mean square error defined by $err = \frac{\|\chi-\tilde{\chi}\|^2}{\|\chi\|^2}$, where χ is the actual contrast profile and $\tilde{\chi}$ the estimated one.

In the first example, shown in fig. 1(a), the task is the reconstruction of five lossless point-like targets. The imaging domain is discretized into 46×46 square cells [18], while the inverse problem grid is 23×23 cells. Moreover, $L = 2\lambda$, N=M=21 and SNR = 10dB. By estimating the target support, fig. 1(b), it is possible to choose the more suitable inversion approach. Accordingly, the reconstruction obtained by means of eq. (6) is reported in fig. 1(c)-(d). As it can be seen, the joint exploitation of virtual experiments and CS allow a very accurate reconstruction. In order to understand the roles played by synthetic experiments and field approximation respectively, in fig.1(e)-(f) we report the reconstruction obtained using synthetic experiments and approximating the internal field with the incident one. As it can be seen, reconstructions appear to be considerably worse. Notably, exploitation of the standard Born Approximation to the original data yields completely unreliable results.

In the second example, three lossless squares embedded in a domain of side $L = 3\lambda$ are considered. The domain is discretized into 50×50 cells and the SNR is 20 dB. Moreover, N=M=26. As the scatterers are not sparse in the pixel basis, see fig. 2(b), we use the approach (7) to retrieve the unknown profile. The result agrees with the reference contrast profile, see fig. 2(c)-(d).

As last example, the lossy profile reported in fig. 3(a)-(b) has been considered. In this example, N=M=21, $L = 2\lambda$, $N_c = 32 \times 32$ and SNR $= 20\,dB$. Also in this case, the CS based approach (7) allows to obtain a nearly optimal reconstruction of the contrast profile, see fig. 3(d)-(e).

V. Conclusion

In this letter, we have shown that it is possible to considerably enlarge the applicability of CS to microwave imaging by taking advantage of a recently introduced approach to inverse scattering based on the concept of virtual experiments. In such a framework, a convenient total field approximation holds true, which hence allows to successfully consider within the usual CS theory (which just holds true for linear problems) a considerably wider class contrast profiles. In particular, as show by reported examples, the reconstruction of non-weak scatterers, which are also non sparse in the common pixel

based representation, is now possible.

REFERENCES

[1] Donoho D., "Compressed sensing," *IEEE Trans. Inf. Theory*, 52(4): 1289–1306, 2006

[2] R. G. Baraniuk, "Compressive sampling," *IEEE Signal Process. Mag.*, 24(4): 118-124, Jul. 2007.

[3] L. Poli, G. Oliveri, and A. Massa, "Microwave imaging within the first-order Born approximation by means of the contrast-field Bayesian compressive sensing," *IEEE Trans. Antennas Propag.*, 60(6): 2865–2879, Jun. 2012.

[4] G. Oliveri, L. Poli, P. Rocca, and A. Massa, "Bayesian compressive optical imaging within the Rytov approximation," *Opt. Lett.*, 37(10): 1760–1762, 2012.

[5] M. Azghani, P. Kosmas, F. Marvasti, "Microwave imaging based on compressed sensing using adaptive thresholding", *In Proc. of the 8-th European Conference on Antennas and Propagation (EUCAP)*, 799–801, IEEE, 2014.

[6] Oliveri, G.; Anselmi, N.; Massa, A, "Compressive Sensing Imaging of Non-Sparse 2D Scatterers by a Total-Variation Approach within the Born Approximation," *Antennas and Propagation, IEEE Transactions on*, 2014.

[7] L. Crocco, I. Catapano, L. Di Donato, and T. Isernia, "The linear sampling method as a way for quantitative inverse scattering", *IEEE Trans. Antennas Propag.*, 4(60):1844–1853, 2012.

[8] O. M. Bucci and T. Isernia, "Electromagnetic inverse scattering: retrievable information and measurement strategies" *Radio Sci.*, 32:2123–2138, 1997.

[9] O. M. Bucci, L. Crocco, and T. Isernia, "Improving the reconstruction capabilities in inverse scattering problems by exploitation of close-proximity setups", *J. Opt. Soc. Am. A*, 16: 1788-1798,1999.

[10] D. Colton, H. Haddar, and M. Piana, "The linear sampling method in inverse electromagnetic scattering theory", *Inverse Probl.*, 19:105–137, 2003.

[11] I. Catapano, L. Crocco, and T. Isernia, "On simple methods for shape reconstruction of unknown scatterers" *IEEE Trans. Antennas Propag.*, 55:1431–1436, 2007.

[12] M. Bevacqua, S. Scapaticci, "Exploiting Compressive Sensing in MNP enhanced MWI for breast cancer imaging", *In Proc. of the XX Riunione Nazionale di Elettromagnetismo - RiNEm 2014*, Padova, Italy, 2014.

[13] G. Bellizzi, O. M., Bucci, and I. Catapano, "Microwave cancer imaging exploiting magnetic nanoparticles as contrast agent", *IEEE Trans. Biomed. Eng.*, 58(9): 2528-2536, 2011.

[14] F. Ahmad and M. G. Amin, "Through-the-Wall Human Motion Indication Using Sparsity-Driven Change Detection", *IEEE Trans. on Geosci. Remote Sens.*, 51: 881-890, 2013.

[15] R. Scapaticci, L. Di Donato, I. Catapano, and L. Crocco, "A feasibility study on microwave imaging for brain stroke monitoring" *Prog. Electromagn. Res. B*, 40:305-324, 2012.

[16] Chen S., Donoho D., M. Saunders D., "Atomic decomposition by basis pursuit," *SIAM J. Sci. Comput.*, 20(1): 33–61, Aug. 1999.

[17] E. J. Candès, M. Wakin, and S. Boyd. "Enhancing sparsity by reweighted l1 minimization," *J. Fourier Anal. Appl.*, 2008.

[18] J. Richmond, "Scattering by a dielectric cylinder of arbitrary cross section shape", *IEEE Trans. Antennas Propag.*, 13(3):334-341, 1965.

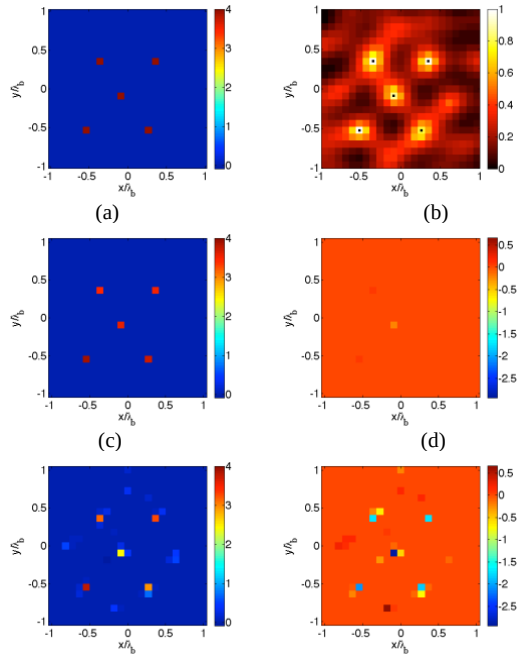

Fig. 1. The five point-like scatterers. (a) Contrast reference profile. (b) Normalized logarithmic LSM indicator with the selected pivot points superimposed as dots. The retrieved profile with approach (6) ($\delta = 0.15\,\|\boldsymbol{y}\|_{\ell_2}$ and *err*=0,26%): (c) real and (d) imaginary part. The retrieved profile with approach (6) ($\delta = 0.15\,\|\boldsymbol{y}\|_{\ell_2}$ and *err*=10%) in conjunction with Born approximation and the virtual experiments: (e) real and (f) imaginary part.

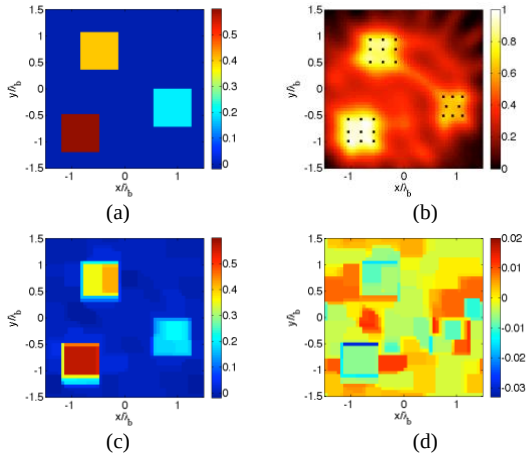

Fig. 2. The three squares. (a) Contrast reference profile. (b) Normalized logarithmic LSM indicator with the selected pivot points superimposed as dots. The retrieved profile with approach (7) ($\delta = 0.23\,\|\boldsymbol{y}\|_{\ell_2}$ and *err*=8%): (c) real and (d) imaginary part.

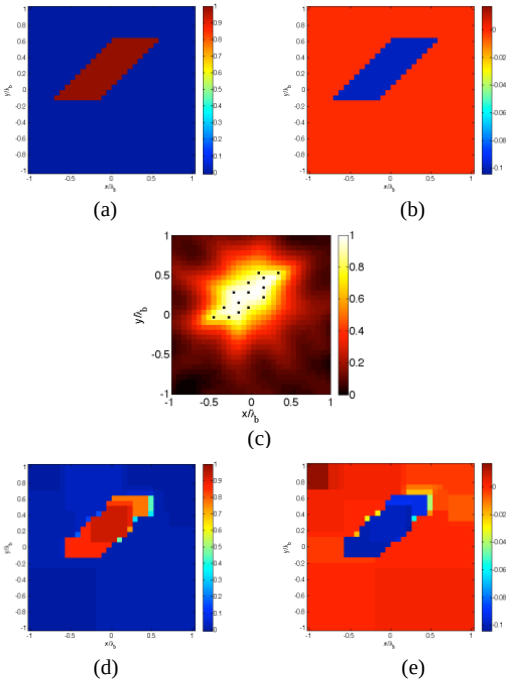

Fig. 3. The parallelogram. Contrast reference profile: (a) real part and (b) imaginary part. (c) Normalized logarithmic LSM indicator with the selected pivot points superimposed as dots. The retrieved profile with approach (7) ($\delta = 0.16\,\|\boldsymbol{y}\|_{\ell_2}$ and *err*=11%): (d) real and (e) imaginary part.